First-principles calculations of structural, elastic and electronic properties of Nb$_2$SnC under pressure

M. Romero, R. Escamilla [*]

Instituto de Investigaciones en Materiales, Universidad Nacional Autónoma de México, Apartado Postal 70-360, México D.F. 04510, Mexico

ARTICLE INFO

ABSTRACT

The structural, elastic and electronic properties of Nb$_2$SnC under pressure were investigated by using first-principles plane-wave pseudo-potential density functional theory within the generalized gradient approximation (GGA). We find that the compressibility along the c-axis was lower than along the a-axis for pressures lower than 4 GPa, while the elastic constants, elastic modulus and the Debye temperature θ_D of Nb$_2$SnC increase monotonically as the pressure increases. Finally, the density of states (DOS) at the Fermi level decreases with increasing pressure, due to the decrease of the contribution of Nb $4d$ states at the Fermi level.

1. Introduction

Ternary carbides and nitrides M$_{n+1}$AX$_n$ (MAX-phases), where n = 1, 2, or 3 refers to 211, 312, and 413 crystal structures, respectively, have recently been the subject of much research [1–3]. M denotes an early transition metal, A is a metametal (a group IIIA or IVA element), and X is either carbon or nitrogen [4]. These layered ternary compounds exhibit a technologically important combination of metallic and ceramic properties, with high strength and stiffness at high temperatures, resistance to oxidation and thermal shock. In addition, they present high electrical and thermal conductivities [5]. These macroscopic properties are closely related to the underlying electronic and crystal structures of the constituent elements and their stacking sequence.

In this family of carbines, only six low-temperature superconducting materials have been discovered: Mo$_2$GaC (T_c = 4 K [6]), Nb$_2$SC (T_c = 5 K [7]), Nb$_2$SnC (T_c = 7.8 K [8]), Nb$_2$AsC (T_c = 2 K [9]), Ti$_2$InC (T_c = 3 K [10]), and Nb$_2$InC (T_c = 7.5 K [11]). Let us note that for the majority of the other MAX phases experimental or theoretical researches of their superconductivity are still absent.

Elastic properties of solids are closely related to many fundamental solid state properties, such as equation of state EOS, specific heat, thermal expansion, Debye temperature, Gruneisen parameter and melting point. From the elastic constants, one can obtain valuable information about the binding characteristics between adjacent atomic planes, the anisotropic character of the bonding, and

the structural stability. On the other hand, the behavior of these materials under pressure, based on calculations or measurements, has become quite interesting in the recent years as it provides insight into the nature of the solid-state theories and determines the values of fundamental parameters.

In the present paper, we would like to deepen our understanding of these systems under pressure by the determination of their structural, elastic, electronic properties, using first-principles plane-wave pseudopotential density functional theory within the generalized gradient approximation (GGA). The paper is organized as follows: in Section 2, we give the technical details of the employed methods. Section 3 is devoted to the structural properties. In Section 4, we present our calculations of elastic constants, the bulk and shear moduli, derived from Voigt–Reuss–Hill approach using both methods. Mechanical properties of the polycrystalline state are also derived. We have left for Section 5 the electronic and the bonding nature of these compounds. Finally, we summarize our main finding in Section 6.

2. Methods of calculation

The calculations presented in this work were performed by employing the Cambridge Serial Total Energy Package software (CASTEP), with the plane wave pseudopotential code [12,13]. The correlation functional GGA-PW91 [14] was used in the calculations plane-wave basis set with 360 eV energy cut-off. For the sampling of the Brillouin zone a Monkhorst–Pack grid [15] of 9 × 9 × 8 k-points was employed. The convergence tolerances were set as follows: 10^{-6} eV/atom for the total energy, 0.002 eV/Å for the

* Corresponding author. Tel.: +52 5 622 4635; fax: +52 5 616 1251.
E-mail address: rauleg@unam.mx (R. Escamilla).

Table 1
Structural parameters of Nb_2SnC compound under pressure.

|	Pressure (GPa)	a (Å)	c (Å)	c/a	z	Unit cell-volume (Å^3)
	0.0	3.263	13.906	4.262	0.0821	128.25
	2.0	3.254	13.827	4.249	0.0823	126.77
	4.0	3.237	13.817	4.268	0.0827	125.41
	6.0	3.223	13.772	4.273	0.0830	124.10
	8.0	3.214	13.730	4.272	0.0832	122.85
	10.0	3.203	13.688	4.273	0.0836	121.64
Exp.[a]	0.0	3.220	13.707	4.26	0.0830	123.08
Calc.[b]	0.0	3.2006	13.5345	4.2287	0.0846	120.07

[a] Ref. [8].
[b] Ref. [16].

maximum force on atoms, 10^{-4} Å for the maximum atomic displacement, and 0.003 for the maximum strain amplitude.

3. Geometry and structure optimization

The considered superconducting Nb_2SnC phase possess the hexagonal structure with a space group $P6_3/mmc$ (No. 194), where blocks of transition metal carbides [NbC] (formed by edge-shared Nb_6C octahedra) are sandwiched with Sn atomic sheets. The Wyckoff positions of atoms in Nb_2SnC are C: 2a (0,0,0), Sn: 2d (1/3,2/3,3/4), and Nb atoms: 4f (1/3,2/3,z), where z is 0.083.

The calculated equilibrium structural parameters of the Nb_2SnC compound under pressure are shown in Table 1, together with other theoretical results [16,?] and experimental data [8]. In Fig. 1a, we exhibit the pressure dependence of the normalized lattice parameters c/a, a/a_0, and c/c_0 as well as the normalized volume V/V_0 (where a_0, c_0, and V_0 are the zero pressure equilibrium structural parameters [8]). The normalized intermolecular distances r_1/r_{10} and r_2/r_{20} (where r_{10} and r_{20} are the zero pressure equilibrium distances of Nb–Sn and Nb–C, respectively) are shown in Fig. 1b.
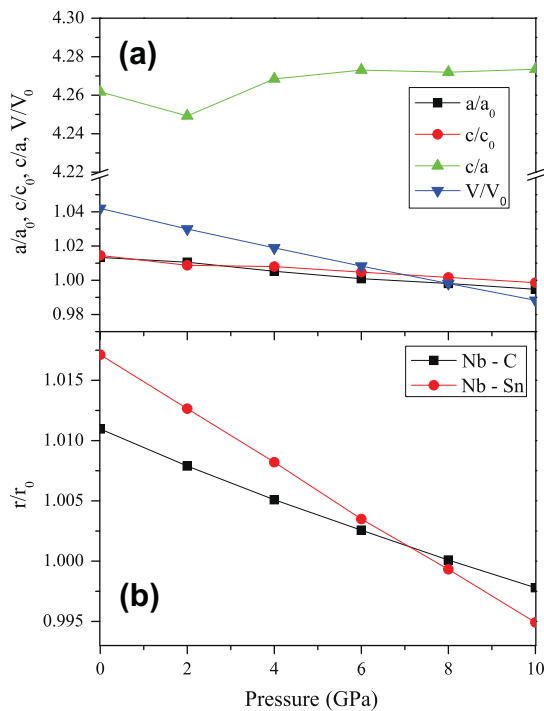
Fig. 1. (a) The normalized volume V/V_0, a/a_0, c/c_0, and c/a as a function of pressure at $T = 0$ and (b) variation of the normalized distance r/r_0 between the atoms with pressure.

We notice in Fig. 1a that, when pressure increases, the equilibrium ratio c/a ranges from 4.262 at 0 GPa to 4.249 at 2 GPa, a decrease of about 0.30%; however, when pressure rises from 4 to 10 GPa, the increase is 0.11%. Therefore, the compressibility along the c-axis was lower than along the a-axis in the basal plane for pressures lower than 4 GPa. Data shown in Fig. 1b indicate that the curve of r_1/r_{10} (the distance between the Nb atom and the Sn atom) becomes steeper than the corresponding one of r_2/r_{20}, as pressure increases, indicating that the direction along Nb–Sn is more easily compressed. These results are in agreement with weaker Nb–Sn bonds that determine the size c lattice parameter. Moreover, the atoms in the interlayers become closer, and the interactions between them becomes stronger; contractions of Nb–Sn and Nb–C interatomic distances under pressure result in the change of bonding anisotropy of Nb_2SnC structure, which induces the variety of electronic structure.

4. Elastic stiffness tensor calculation

The structure of Nb_2SnC compound is hexagonal and there are six elastic stiffness constants, C_{11}, C_{12}, C_{13}, C_{33}, C_{44}, and C_{66} [18], five of them are independent since $C_{66} = (C_{11} - C_{12})/2$. Because a polycrystalline material can be treated as an aggregate of single crystals at random orientation, there will be two possible extreme cases for external load, known as: Voigt and Reuss approximation [19,20]. The former means that a uniform strain in a polycrystal is equal to the applied external strain while the latter indicates the equality of the uniform stress to the external stress. For hexagonal lattices, the Reuss and Voigt shear (G_R and G_V) and the Reuss and Voigt bulk modulus (K_R and K_V) can be defined as:

$$G_R = \frac{5}{2} \frac{C_{44}C_{66}\left[C_{33}(C_{11} + C_{12}) - 2C_{13}^2\right]}{3K_V C_{44}C_{66} + (C_{44} + C_{66})\left[C_{33}(C_{11} + C_{12}) - 2C_{13}^2\right]} \tag{1}$$

$$G_V = \frac{1}{30}(C_{11} + C_{12} + 2C_{33} - 4C_{13} + 12C_{44} + 12C_{66}) \tag{2}$$

$$K_R = \frac{C_{33}(C_{11} + C_{12}) - 2C_{13}^2}{C_{11} + C_{12} + 2C_{33} - 4C_{13}} \tag{3}$$

$$K_V = \frac{1}{9}[2(C_{11} + C_{12}) + C_{33} + 4C_{13}] \tag{4}$$

Consequently, the elastic moduli of the polycrystalline material can be approximated by Hill's average [21]: $G = \frac{1}{2}(G_R + G_V)$ for shear moduli and $K = \frac{1}{2}(K_R + K_V)$ for bulk moduli. Using these values, the Young's modulus, E, and Poisson's ratio, σ, can be obtained by:

$$E = \frac{9KG}{3K + G} \tag{5}$$

and

$$\sigma = \frac{3K - 2G}{2(3K + G)} \tag{6}$$

In order to measure the elastic anisotropy of polycrystalline samples, we have calculated the percentage of anisotropy for the bulk and shear moduli. They are defined as [22]:

$$A_K = (100)\frac{K_V - K_R}{K_V + K_R} \tag{7}$$

and

$$A_G = (100)\frac{G_V - G_R}{G_V + G_R} \tag{8}$$

These values can range from zero (isotropic) to 100%, the maximum anisotropy.

As an important fundamental parameter, the Debye temperature (θ_D) is closely related to many physical properties of solids such as the specific heat and the melting temperature. One of the standard methods to calculate the Debye temperature is from elastic constants data, since θ_D may be estimated from the average sound velocity (v_m), by the following equation [23],

$$\theta_D = \frac{h}{k} \left[\frac{3n}{4\pi} \left(\frac{N_A \rho}{M} \right) \right]^{1/3} v_m, \quad (9)$$

where h is Plank's constant, k is Boltzmann's constant, N_A is Avogadro's number, ρ is the density, M is the molecular weight and n is the number of atoms in the molecule. The average sound velocity v_m is given by:

$$v_m = \left[\frac{1}{3} \left(\frac{2}{v_t^3} + \frac{1}{v_l^3} \right) \right]^{-1/3}, \quad (10)$$

where v_l and v_t are the longitudinal and transverse elastic wave velocities, respectively, which are obtained from Navier's equations as follows [24]:

$$v_l = \sqrt{\frac{3K + 4G}{3\rho}} \quad (11)$$

and

$$v_t = \sqrt{\frac{G}{\rho}}, \quad (12)$$

where ρ is the density, K is the bulk modulus and G is the shear modulus.

The mechanically stable phases or macroscopic stability are dependent on the positive definiteness of stiffness matrix [25]. For hexagonal lattices, must be carry out the conditions known as the Born criteria [26]: $C_{11} > 0$, $(C_{11} - C_{12}) > 0$, $C_{44} > 0$ and $(C_{11} + C_{12})C_{33} - 2C_{13}^2 > 0$. Our elastic constants calculations, shown in Table 2, completely satisfy the above conditions, indicating that the hexagonal phase of the Nb$_2$SnC compound is mechanically stable. Moreover, our values are consistent with previously reported values [16,17]. The brittleness of these compounds is indicated by the small values of C_{12} and C_{13} among all the five constants. Both the large (C_{13}/C_{12}) ratio and the small (C_{33}/C_{11}) one indicate that the atomic bonding length along the *a*-axis is stronger than the one corresponding to the *c*-axis; this fact is consistent with the crystal structure of the Nb$_2$SnC compound which is a layered-type with the layers perpendicular to the *c*-axis.

The hardness of a material is defined by its elastic moduli: bulk modulus (K), a measure of resistance to volume changes by applied pressure, and shear modulus (G), a measure of resistance to reversible deformations upon shear stress [27]. Generally, the search for hard materials is simplified by searching for materials with large bulk modulus or shear modulus, because there is a direct relation between bulk modulus, shear modulus and hardness [28].

Fig. 2 shows the K and G elastic moduli and unit cell-volume as a function of pressure. We can observed that K and G increase while the unit cell-volume decreases under pressure, meaning that the hardness and the compression of the material increases under pressure. At 0 GPa, the bulk modulus of Nb$_2$SnC compound (237 GPa) is slightly higher than the corresponding for others well known superconducting materials, such as MgB$_2$ ($K = 139.3$ GPa), MgCNi$_3$ (170.4 GPa),YBCO (138 GPa) and YNi$_2$B$_2$C (200 GPa) [29–32].

An evaluation criterion of ductility or brittleness of a material, is through of the ratio K/G, according to this criterion a $K/G < 1.75$ implies that the material is brittle [33]. From Table 2 it is evident that the Nb$_2$SnC compound is not brittle. On the other hand, in order to determine through elastic properties if our material is covalent or

Table 2
Elastic constants (C_{ij}), bulk modulus (K), shear modulus (G),Young modulus (E), Poisson's ratio (v) and percentage of anisotropy for the bulk (A_K) and shear (A_G) of Nb$_2$SnC compound under pressure.

	Pressure (GPa)	C_{11}	C_{12}	C_{13}	C_{33}	C_{44}
	0.0	286.5	91.5	126.8	288.5	99.8
	2.0	298.5	96.3	133.7	297.1	109.9
	4.0	311.7	101.0	136.8	306.3	115.6
	6.0	323.6	106.7	140.6	308.9	120.0
	8.0	332.0	110.5	145.1	316.1	124.0
	10.0	338.7	112.7	148.8	321.5	129.5
Calc.[a]	0.0	315	99	141.0	309.0	124.0
Calc.[b]	0.0	254.8	100.8	120.0	243.0	58.9

	Pressure (GPa)	K (GPa)	G (GPa)	K/G	E (GPa)	v	A_K	A_G
	0.0	171.1	93.3	1.83	236.9	0.271	0.200	0.678
	2.0	179.9	98.6	1.82	250.1	0.270	0.176	0.993
	4.0	186.3	103.3	1.80	261.6	0.266	0.115	0.963
	6.0	192.3	106.5	1.81	269.6	0.266	0.043	1.054
	8.0	197.9	109.1	1.81	276.6	0.267	0.040	1.130
	10.0	202.1	112.2	1.80	284.0	0.265	0.039	1.314
Calc.[b]	0.0	171.1	66.8	–	177.3	0.33	–	–

[a] Ref. [16].
[b] Ref. [17].

metallic we have considered the Poisson Ratio criterion (v)[34], covalent materials $v = 0.1$ and metallic ones is between 0.25 and 0.35. In our case, the value of v is around 0.27 (see Table 2), which is indicative of metallic contribution in intra-atomic bonding. However this character decreases under pressure.

The Debye temperature calculated from the elastic constants at different pressures, is shown in the Table 3. We observe that the Debye temperature increases under compression due to stiffening of the lattice. It is well known that phonon stiffening will reduce electron phonon coupling constant and hence T_c (see Fig. 3). The comparison of the θ_D of Nb$_2$SnC obtained at 0 GPa with those reported by others, show us that our value is similar to the calculated by Anderson [23] and Kanoun et al. [35] but, is significantly higher than the one reported by Lofland et al. [36].

5. Electronic and bonding properties under pressure

Finally, the effects of pressure on the density of states (DOS) of Nb$_2$SnC are examined, for pressures varying in the range from 0 to 10 GPa. Fig. 4a displays the pressure dependence of the total density of states of Nb$_2$SnC near the Fermi level, (vertical line is the Fermi level E_F). The calculated equilibrium density of states
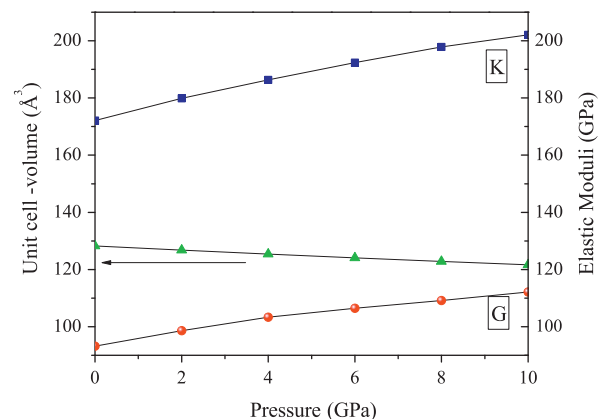

Fig. 2. Unit cell-volume, K and G elastic moduli of Nb$_2$SnC compound under pressure.

Table 3
Debye temperature (θ_D) and velocity of sound (v_m) of Nb$_2$SnC compound under pressure.

	Pressure (GPa)	v_m (m/s)	(θ_D)
	0.0	3569.7	421.5
	2.0	3647.3	432.3
	4.0	3710.8	441.4
	6.0	3747.8	447.4
	8.0	3776.3	452.3
	10.0	3808.0	457.6
Calc.[a]	0.0	–	469
Calc.[b]	0.0	–	479.70, 511.74
Exp.[c]	0.0	-	380
Exp.[d]	0.0	-	324

[a] Ref. [16].
[b] Ref. [35]. (Using FP-LAPW and PP-PW respectively).
[c] Ref. [36].
[d] Ref. [37].

at the Fermi level E_F ($P = 0$ GPa) is 3.44 electrons/eV, which is in agreement with those reported by others [35]. Fig. 4b shows the partial densities of states (PDOS) of the d electrons of Nb and the p electrons of Sn and C at $P = 0$ and 10 GPa. Hence, we may conclude that Nb$_2$SnC is a better conductor a zero pressure. Our understanding of this behavior can be improved by examination of the partial densities of states PDOS at 0 GPa in the Fig. 4b. In the energy range from -7 to -1.5 eV, the C $2p$ PDOS has the same shape as the $4d$ electronic states of Nb atoms located between C layers. It is indicative of a hybridization between Nb $4d$ and C $2p$ states and thus of a covalent interaction. In the energy range from -1.7 to -0.2 eV, the Sn $5p$ states interact mainly with the Nb $4d$ states. The energy of the Sn $5p$–Nb $4d$ hybrids is higher in energy than the C $2p$–Nb $4d$ ones (i.e. closer to the Fermi level) suggesting that Nb–C bonds are stronger than Nb–Sn bonds. It is this strong C $2p$–Nb $4d$ hybridization which stabilizes the structure of Nb$_2$SnC, a general trend in MAX phases. We may describe the bonding picture in Nb$_2$SnC as a mixture of covalent, metallic and ionic interactions. In addition the above mentioned covalent Nb–C and Nb–Sn bonds, the metallic-like Nb–Nb bonding occurs owing to the overlap of the near – Fermi Nd $4d$ states, the mentioned ionic contribution is due to the difference in electronegativity between the compressing elements: Nb (1.60), C (2.55) and Sn (1.96). In the vicinity of the Fermi level, Nb $4d$ states dominate and should contribute to the conduction properties of Nb$_2$SnC. According to the results of our calculations, an increase in the pressure leads to a decrease in the DOS $N_{Nb}(E_F)$ associated with the niobium states at the Fermi level, while the DOS $N_C(E_F)$ and $N_{Sn}(E_F)$ associated with the carbon and tin states at the Fermi level remain virtually unchanged (see Fig. 4b).
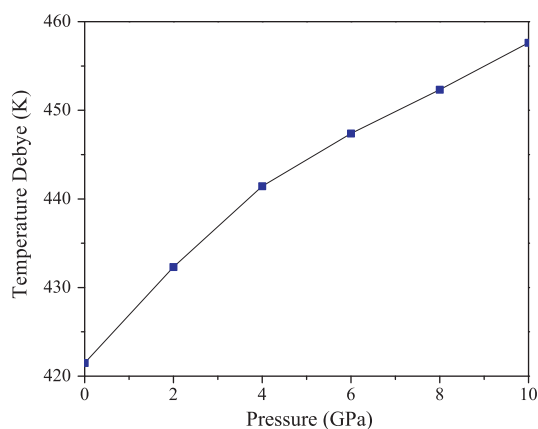
Fig. 3. Debye temperature θ_D of Nb$_2$SnC compound under pressure.
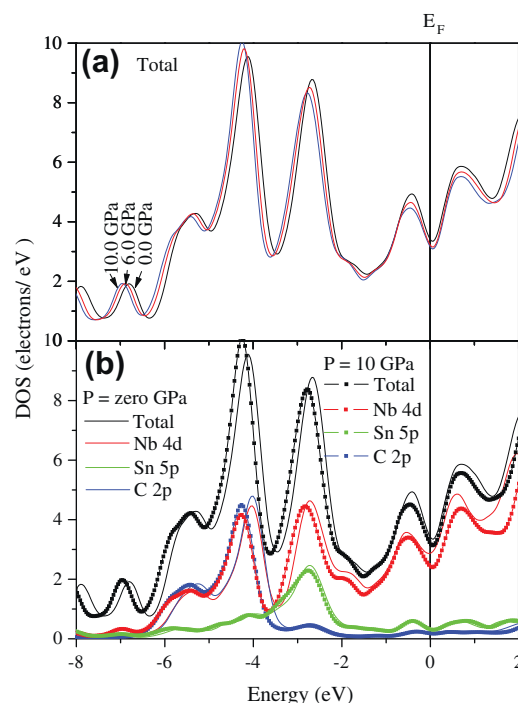
Fig. 4. (a) The total DOS of Nb$_2$SnC under pressure and (b) the partial DOS of p and d electrons of Nb$_2$SnC at $P = 0$ and 10 GPa.

As a consequence, at 10 GPa the density of states at the Fermi level E_F decreases around of 9.2% respect to 0 GPa. This behavior is similar to one observed in MgB$_2$ [38]. The DOS at the Fermi level is an important parameter known to affect the superconducting transition temperature T_c. Judging from Bardeen–Cooper–Schrieffer superconducting theory, the reduction of the density of states at the Fermi level shows that the transition temperature T_c decreases as pressures increases [39].

6. Conclusions

In summary, the structural, elastic and electronic properties of Nb$_2$SnC under pressure have been investigated using planewave pseudopotential density functional theory within the generalized gradient approximation (GGA). We find that the effect of pressure on the crystal structure reflects in a compression of the unit cell-volume, more easily along the c-axis than on the a-axis for pressures higher than 4 GPa. We also observed, that the elastic constants and elastic modulus increase monotonically. As a consequence, the hardness and the compression of the material increase under pressure. Using the elastic constants the Debye temperature θ_D was calculated and we found that it increases under pressure. Finally, according to the results of our calculations, an increase in the pressure would lead to a decrease in the density of states (DOS) of Nb$_2$SnC, due mainly to the decrease of the PDOS associated with the niobium states at the Fermi level.

References

[1] V.H. Nowtony, Prog. Solid State Chem. (1971) 5 27.
[2] W. Jeitschko, H. Nowotny, Monatsh. Chem. 98 (1967) 329.
[3] H. Wolfsgruber, H. Nowotny, F. Benesovsky, Monatsh. Chem. 98 (1967) 2403.
[4] M.W. Barsoum, Metall. Mater. Trans. A 30 (1999) 1727.
[5] M.W. Barsoum, Prog. Solid State Chem. 28 (2000) 201.
[6] L.E. Toth, J. Less Common Met. 13 (1967) 129.
[7] K. Sakamaki, H. Wada, H. Nozaki, Y. Onuki, M. Kawai, Solid State Commun. 112 (1999) 323.
[8] A.D. Bortolozo, O.H. Sant-Anna, M.S. da Luz, C.A.M. dos Santos, A.S. Pereira, K.S. Trentin, A.J.S. Machado, Solid State Commun. 139 (2006) 57.
[9] S.E. Lofland, J.D. Hettinger, T. Meehan, A. Bryan, P. Finkel, S. Gupta, M.W. Barsoum, G. Hug, Phys. Rev. B 74 (2006) 174501.
[10] A.D. Bortolozo, O.H. Sant-Anna, C.A.M. dos Santos, A.J.S. Machado, Solid State Commun. 144 (2007) 419.
[11] A.D. Bortolozo, Z. Fisk, O.H. Sant'Anna, C.A.M. dos Santos, A.J.S. Machado, Physica C 469 (2009) 256.
[12] M.C. Payne, M.P. Teter, D.C. Allan, T.A. Arias, J.D. Joannopoulos, Rev. Mod. Phys. 64 (1992) 1045.
[13] M. Segall, P.J. Lindan, M. Probert, C. Pickard, P. Hasnip, S. Clark, M.J. Payne, Phys.: Condens. Matter 14 (2002) 2717.
[14] J.P. Perdew, Y. Wang, Phys. Rev. B 45 (1992) 1324.
[15] H.J. Monkhorst, J.D. Pack, Phys. Rev. B 13 (1976) 5188.
[16] A. Bouhemadou, Physica B 403 (2008) 2707.
[17] Igor R. Shein, Alexander L. Ivanovskii, Phys. Status Solidi B 1 (2011) 228.
[18] J.F. Nye, Physical Properties of Crystals, Claredon, Oxford, 1985.
[19] W. Voigt, Lehrbuch der Kristallphysik, Taubner, Leipzig, 1928, p. 739.
[20] A. Reuss, Z. Angew, Math. Mech. 9 (1929) 49.
[21] R. Hill, Proc. Phys. Soc. 65 (1952) 349.
[22] D.H. Chung, W.R. Buessem, F.W. Vahldiek, Anisotropy in Single Crystal Refractory Compounds, Plenum, New York, 1968, (S.A. Mersol) p. 217.
[23] O.L. Anderson, Phys. Chem. Solids 24 (1963) 909.
[24] E. Schreiber, O.L. Anderson, N. Soga, Elastic Constants and their Measurements, McGraw-Hill, New York, 1973.
[25] F.I. Fedoras, Theory of Elastic Waves in Crystals, Oxford University Press, New York, 1985.
[26] M. Born, K. Hang, Dynamical Theory and Experiments I, Springer-Verlag Publishers, Berlin, 1982.
[27] A.F. Young, C. Sanloup, E. Gregoryanz, S. Scandolo, R.J. Hemley, H.-K. Mao, Phys. Rev. Lett. 96 (2006) 155501.
[28] S.-H. Jhi, J. Ihm, S.G. Louie, M.L. Cohen, Nature 399 (1999) 132.
[29] V. Milman, M.C. Warren, J. Phys.: Condens. Matter 13 (2001) 5585.
[30] Wei Zhang, Xiang-Rong Chen, Ling-Cang Cai, Fu-Qian Jing, J. Phys.: Condens. Matter 20 (2008) 325228.
[31] Ming Lei, J.L. Sarrao, W.M. Visscher, T.M. Bell, J.D. Thompson, A. Migliori, U.W. Welp, B.W. Veal, Phys. Rev. B 47 (1993) 6154.
[32] S. Meenakshi, V. Vijayakumar, R.S. Rao, B.K. Godwal, S.K. Sikka, Z. Hossain, R. Nagarajan, L.C. Gupta, R. Vijayaraghavan, Physica B 223–224 (1996) 93.
[33] S.F. Pugh, Phil. Mag. 45 (1954) 833.
[34] J. Haines, J.M. Le?ger, G. Bocquillon, Ann. Rev. Mater. Res. 31 (2001) 1.
[35] M.B. Kanoun, S. Goumri-Said, A.H. Reshak, Comput. Mater. Sci. 47 (2009) 491.
[36] S.E. Lofland, J.D. Hettinger, K. Harrell, P. Finkel, S. Gupta, M.W. Barsoum, G. Hug, Appl. Phys. Lett. 84 (2004) 508.
[37] M.W. Barsouma, T. El-Raghy, W.D. Porter, H. Wang, J.C. Ho, S. Chakraborty, Appl. Phys. 88 (2000) 6313.
[38] F.N. Islam, A.K.M.A. Islam, M.N.J. Islam, Phys.: Condens. Matter 13 (2001) 11661.
[39] J. Bardeen, L.N. Cooper, J.R. Schrieffer, Phys. Rev. 108 (1957) 1175.